

# Large-Scale Oscillations of a Feedstream Inside a Stirred Tank Reactor

Iris L. M. Verschuren, Johan G. Wijers, and Jos T. F. Keurentjes

Eindhoven University of Technology, Dept. of Chemical Engineering and Chemistry, Process Development Group,  
Eindhoven, The Netherlands

*Recent studies have shown feedstreams inside stirred tank reactors to oscillate. When multiple feed points are used, these oscillations can cause feedstreams to overlap. The objective of this study is to determine a description of the oscillations that can be used to prevent the feedstreams to overlap. The oscillations are analyzed by determining the displacements of the centers of the mass of a feedstream in radial cross sections. The growth of the root-mean-square radius of these displacements with time is linear, corresponding to the "initial growth stage." The growth rate of the root-mean-square radius with time proved to equal the velocity fluctuations related to turbulent motions with a size larger than the diameter of the feedstream, indicating that these large-scale turbulent motions are responsible for large-scale oscillations. With the description obtained for the root-mean-square radius, the minimal distance between two feed pipes necessary to prevent the overlap of the feedstreams can be calculated.*

## Introduction

Stirred tank reactors with a feed stream are frequently used in the chemical and biochemical industry. When the reaction is slow compared to the mixing process, the feedstream will be homogeneously mixed before a reaction takes place and the product distribution will only depend on the chemical kinetics. However, when the time scale for the reaction is of the same order of magnitude as the time scale for mixing, the selectivity of a process of competitive reactions will depend on the mixing rate (Rys, 1992).

Because mixing has a large influence on the product quality of fast competitive reactions, various models for feedstream mixing inside stirred tank reactors have been proposed in the literature and feedstream mixing has been the subject of numerous experimental studies. The more recent studies have shown feedstreams inside stirred tank reactors to oscillate (Houcine et al., 1999; Schoenmakers et al., 1997). The mixing models proposed in the literature do not take into account these large-scale oscillations. This is because, generally, the mixing of one feedstream with homogeneous bulk liquid is investigated (for example, Baldyga et al., 1993; Verschuren et al., 2001). Under these circumstances, large-scale oscillations of a feedstream will have no effect on the mixing rate.

A method to optimize the selectivity of mixing sensitive reactions is to use sufficiently low feed flow rates so that the selectivity is controlled by micromixing (Baldyga and Bourne, 1999). By increasing the number of feed points, the feed flow rate can be decreased without decreasing productivity, provided that the feed points are located at hydrodynamically equivalent positions and the feedstreams do not overlap (Baldyga and Bourne, 1999). When the feed points are located closely together, the large-scale oscillations of the feedstreams can cause the feedstreams to come in contact with each other. The objective of this study is to determine a description that can be used to calculate the minimal distance between feed points necessary to prevent feedstreams to overlap.

## Theory

Generally, the diameter of the feedstream inside a stirred tank reactor is much smaller than the length scale of the largest turbulent motions. When this is the case, the feedstream is dispersed by turbulent motions with a size comparable to the diameter of the feedstream (Lesieur, 1990). In this study, we will verify the presumption that the larger turbulent motions, that is, those not taking part in the dispersion process, transport the feedstream bodily, which causes

Correspondence concerning this article should be addressed to I. L. M. Verschuren.

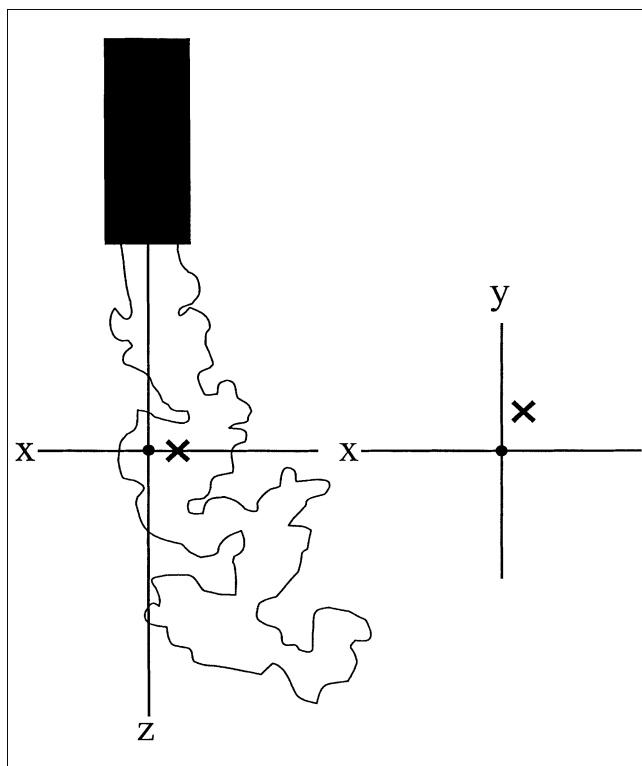


**Figure 1. Center of mass (×) of a radial cross section of a feedstream.**

the feedstream to oscillate. This presumption is founded on literature regarding mixing in the atmosphere, which also describes the spreading of a plume in the atmosphere to be the result of these two processes: the dispersion of the plume by small eddies with a size equivalent to the size of the plume, and the fluctuation of the entire plume around its mean position due to large-scale turbulent motions (Blackadar, 1996).

The oscillations of a feedstream in a stirred tank reactor will be analyzed by determining the displacements of the centers-of-mass of a feedstream in radial cross sections, as illustrated in Figure 1. The turbulent movements of the center-of-mass of a lump of fluid can be considered as a passive marker moving in a turbulent flow field (Baldyga and Bourne, 1999).

The mean square displacement of a large number of passive markers in a stationary and homogeneous turbulent flow field without a mean velocity as a function of time ( $t$ ) is derived by Taylor (1921)

$$\overline{X^2} = 2\overline{u_i'^2} \int_0^t (t - \tau) \rho_{ii}(\tau) d\tau \quad (1)$$

where  $\overline{u_i'^2}$  is the Eulerian mean square turbulent velocity fluctuation in the  $i$ -direction and  $\rho_{ii}$  is the Lagrangian two-time velocity autocorrelation coefficient. This autocorrelation coefficient is defined by

$$\rho_{ii} = \frac{\overline{u_{iL}'(t)u_{iL}'(t+\tau)}}{\overline{u_{iL}'^2}} \quad (2)$$

in which  $u_{iL}'$  is the Lagrangian turbulent velocity fluctuation in the  $i$ -direction. The mean square displacement can be calculated with Eq. 1 when the autocorrelation coefficient is known. Some known features of the autocorrelation coefficient are

$$\rho_{ii}(\tau) = 1 \quad t \rightarrow 0 \quad (3)$$

$$\int_0^\infty \rho_{ii}(\tau) d\tau = T_L \quad (4)$$

where  $T_L$  is the Lagrangian time scale.

Substituting Eq. 3 into Eq. 1 yields the mean square displacement for short dispersion times

$$\overline{X^2} = \overline{u_x'^2} t^2 \quad t \rightarrow 0 \quad (5)$$

This equation shows that for short times the root mean square (rms) displacement is directly proportional to time, with a growth rate equal to the rms fluctuating velocity. A rms displacement directly proportional to time is marked as the “initial growth stage.” Substituting Eq. 4 into Eq. 1 yields the mean square displacement for long dispersion times

$$\overline{X^2} = 2\overline{u_x'^2} T_L t \quad t \rightarrow \infty \quad (6)$$

From Eq. 6, it follows that, for long dispersion times, the rms displacement grows with the square root of time, which is marked as the “random walk regime.”

Consider now the mean square displacement of the center-of-mass of a feedstream in two directions ( $\overline{X^2}$  and  $\overline{Y^2}$ ), as illustrated in Figure 1. The average position of the centers-of-mass obtained by averaging over many centers-of-mass at an axial location is used as the origin of the coordinate system. Therefore, by definition, the mean velocities  $\overline{u_x}$  and  $\overline{u_y}$  are zero. The mean square displacements in each of the two directions are described by Eqs. 5 or 6 given above. The square radius ( $r^2$ ) of the displacements is equal to

$$r^2 = \overline{X^2} + \overline{Y^2} = (\overline{u_x'^2} + \overline{u_y'^2}) \cdot t^2 \quad t \rightarrow 0 \quad (7)$$

$$r^2 = \overline{X^2} + \overline{Y^2} = 2T_L (\overline{u_x'^2} + \overline{u_y'^2}) \cdot t \quad t \rightarrow \infty \quad (8)$$

Taylor's theory describes the mean square displacement of a large number of markers in a turbulence field without a mean velocity. To be able to use this theory, the coordinate system has been chosen so that the mean velocity is zero as described below. The average position of the center-of-mass of a radial cross section of the feedstream is positioned at  $x, y = 0$ . Furthermore, the axial distance below the feed pipe has been replaced by a time scale, using average velocities below the feed pipe. The displacement of a marker in the axial direction ( $z$ ) due to the action of a turbulent motion is assumed to be small compared to the displacement in this direction due to convection with the mean velocity. With this assumption the rms displacement measured at a certain distance  $z$  is equal to the rms displacement at time  $t$  with

$$t = \int_0^z \frac{1}{\overline{u_z}} dz \quad (9)$$

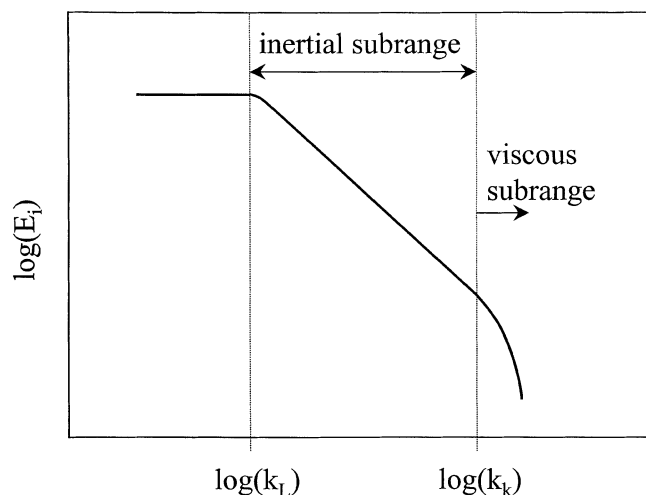


**Figure 2. Energy spectrum of a turbulent velocity signal.**

It has been shown that the hydrodynamics at the location of the feedstream in a stirred vessel with a geometry as used in this study can be described with constant parameters (Verschuren et al., 2001). Therefore, it is concluded that Eqs. 1–8, which are derived for homogeneous turbulence, can be used in this study.

As derived by Taylor (1921), the rms displacement of a passive marker is a function of the velocity fluctuations related to the entire range of turbulent motions. This is to be expected because small-scale, as well as large-scale, turbulent motions move a passive marker in a turbulent flow field. However, only large-scale turbulent motions are assumed to move the center-of-mass of a feedstream. When this is true, not the velocity fluctuations related to the entire range of turbulent motions, but only the velocity fluctuations related to the large-scale turbulent motions ( $\overline{u_{i,LS}^2}$ ) have to be used in Eqs. 5 and 6 to describe the rms displacement of the centers-of-mass.

The distribution of the intensity of the velocity fluctuations over various length scales is given by the energy spectrum of a velocity signal. The one-dimensional (1-D) energy spectrum is defined by

$$\int_0^\infty E_i dk_i = \overline{u_i^2} \quad (10)$$

with  $k_i$  being the wave number in the  $i$ -direction, which is proportional to the reciprocal of an eddy size. An energy spectrum is given in Figure 2. This figure shows three characteristic regions: the low wave number horizontal part which corresponds to the large-scale energy containing eddies, the inertial subrange of wave numbers, and the viscous subrange of wave numbers.

In this study the energy spectrum is measured with Laser Doppler Velocimetry as a function of frequency. This frequency is proportional to the reciprocal of an eddy life time. In the horizontal part in the inertial convective part of an energy spectrum, the spectrum as a function of frequency may

be treated as a rearrangement of the spectrum as a function of wave number, because time scales in these regions are monotonously decreasing with wave number (Tennekes and Lumley, 1972). The velocity fluctuations of the large-scale turbulent motions are calculated from the measured spectra

$$\overline{u_{i,LS}^2} = \int_0^{f_L} E_{i,LS}(f) df \quad (11)$$

in which  $f_L$  is the frequency of the smallest turbulent motions causing the feedstream to oscillate. The frequency of a turbulent motion is given by (Tennekes and Lumley, 1972)

$$f = \frac{u(r)}{2\pi r} \quad (12)$$

in which  $r$  is the radius of a turbulent motion and  $u$  is the velocity of a turbulent motion. In this study the radius of the smallest turbulent motions causing the feedstream to oscillate is assumed to be equal to the radius of the feedstream. The velocity of a turbulent motion in the inertial subrange is (Tennekes and Lumley, 1972)

$$u(r) = C(\epsilon r)^{1/3} \quad (13)$$

where  $\epsilon$  is the local energy dissipation rate and  $C$  is a constant. Experimental data indicate that  $C$  is approximately 1.37 (Rotta, 1972). The local energy dissipation rate at the location of the feed in a stirred vessel with a geometry as used in this study is given by (Verschuren et al., 2001)

$$\epsilon = 0.1 \bar{\epsilon} = 0.1 \frac{N_p N^3 D_{im}^5}{V_{vessel}} \quad (14)$$

in which  $\bar{\epsilon}$  is the average energy dissipation rate,  $N_p$  is the power number equal to 5.3 for the Rushton turbine impeller used in this work (Schoenmakers, 1998),  $N$  is impeller speed,  $D_{im}$  is impeller diameter, and  $V_{vessel}$  is the liquid volume inside the reactor.

## Experimental Studies

The centers-of-mass of a feedstream in radial cross sections have been determined at various axial distances below the feed pipe with Planar Laser Induced Fluorescence (PLIF). The axial distance below the feed pipe has been replaced by a time scale, using average velocities below the feed pipe measured with Laser Doppler Velocimetry. The radius of the smallest turbulent motions causing the feedstream to oscillate is determined from the size of the feedstream visible in the pictures taken with PLIF. To calculate the rms displacements of the centers-of-mass with the equations given above, information on the turbulent velocity fluctuations needs to be available. These velocity fluctuations have been obtained from LDV-experiments. These PLIF and LDV experiments are described in a previous article (Verschuren et al., 2002). The geometry of the vessel and some additional PLIF data processing is described below.

### Geometry of the vessel

The geometry of the vessel used for the PLIF and LDV experiments is given in Figure 3. The vessel was made of Perspex, and had a flat top and bottom and a height equal to the diameter. The internal diameter of the vessel was 0.288 m. The vessel was equipped with four baffles, a feed pipe, an effluent pipe, and a Rushton turbine impeller. The feed pipe internal diameter was 0.008 m. Details of the stirrer geometry are given in Figure 4.

### Processing of data acquired with PLIF

The centers-of-mass of the feedstream were determined for each of the recorded images. First, each gray value image was converted into a concentration image in which the gray-scale is directly related to the concentration. These concentrations were normalized using the initial Fluorescein concentration of the feed liquid and images were reconstructed by assigning a gray-value to each pixel according to

$$G = \frac{C}{C_0} 200 \quad (15)$$

From a converted image, the center-of-mass was determined automatically using the commercially available image analysis program Optimas. This program provides algorithms for image analysis. The following sequence of algorithms was used to determine the center-of-mass. To clearly define the areas containing feed liquid against the background in each image,

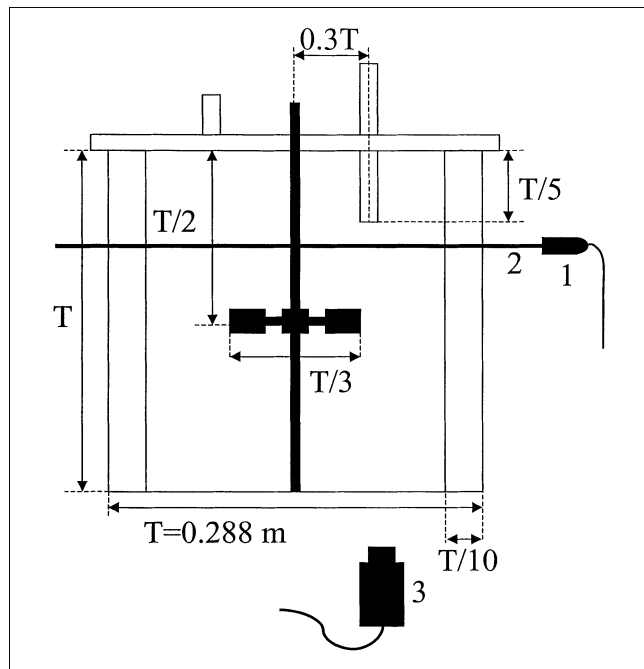


**Figure 3. Geometry of the stirred vessel and the experimental setup used for the planar laser induced fluorescence experiments with (1) laser probe, (2) laser light sheet, and (3) high speed CCD camera.**

the threshold function was used to set a range of values as the foreground. Areas containing feed liquid were detected using the "CreateArea" function. The center-of-mass of the feedstream was determined automatically as the gray-value-weighted center-of-mass from the created areas. When multiple areas were present the gray-value-weighted center-of-mass from the largest area was used. Two typical examples of PLIF images showing areas containing feed liquid and the gray-value-weighted center-of-mass of the largest areas are given in Figure 5.

The origin of the coordinate system was taken equal to the average position of the centers-of-mass obtained by linearly averaging over the 2,000 centers-of-mass per experiment. The rms radius of the displacements was calculated from the  $X$  and  $Y$  coordinates of the centers-of-mass

$$r = \sqrt{\frac{\sum_{i=1}^n X^2}{n} + \frac{\sum_{i=1}^n Y^2}{n}} \quad (16)$$

where  $n$  is the number of images per experiment.

### Results and Discussion

Figures 6 and 7 show the mean and rms fluctuating velocities normalized to the tip speed as a function of the axial coordinate below the feed pipe. From Figure 6, it is concluded that the average axial velocity is approximately equal to 0.16 times the tip speed, independent of position. Figure 7 shows the axial, radial, and tangential rms fluctuating velocities to be approximately equal to 0.05, 0.06, and 0.07 times the tip velocity. In this figure no significant variation of the velocity fluctuations with axial coordinate is observed. Therefore, it is concluded that usage of Taylor's theory derived for homogeneous turbulence is justified.

The size of the smallest turbulent motions causing the feedstream to oscillate is assumed to be equal to the radius of the feedstream. The local radius of the feedstream is determined from the images obtained with PLIF. Typical examples of these images measured at a stirrer speed of 3 Hz are given in Figure 5. These images show cross sections of the feedstream with a radius comparable to the radius of the feed

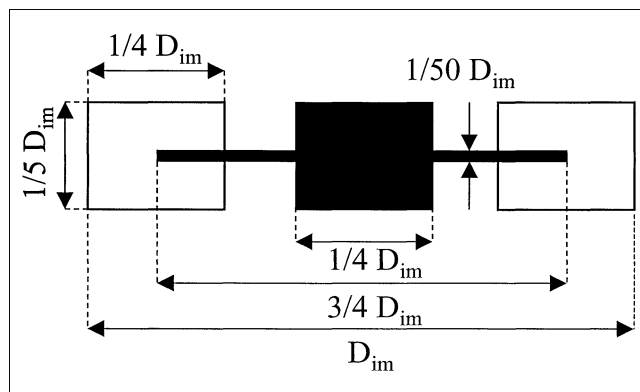


**Figure 4. Details of the impeller geometry.**

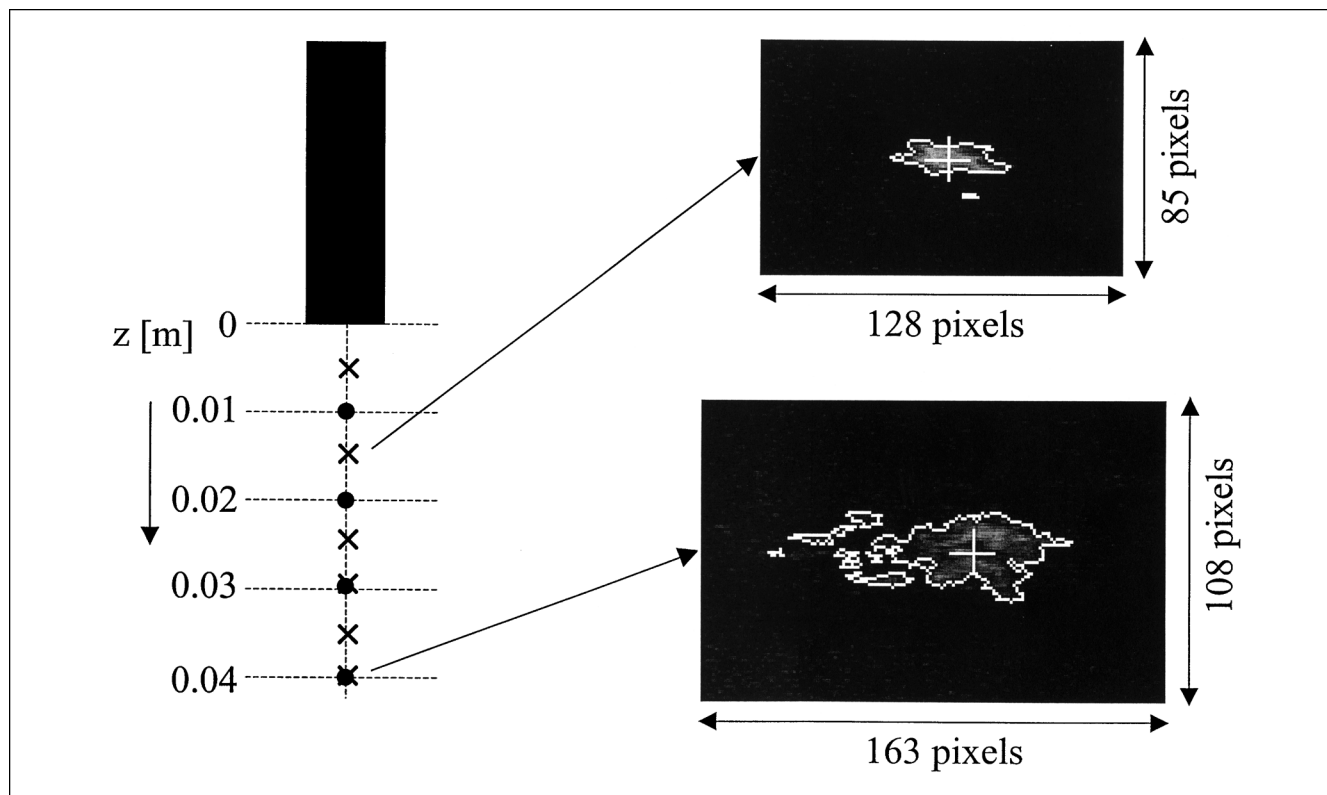


**Figure 5. Measurement positions (●) used for the LDV-experiments and PLIF-experiments (×) and PLIF-images of radial cross sections of a feedstream in a stirred tank reactor measured at a stirrer speed of 3 Hz.**

These images show the gray-value weighted center of mass of the largest created area (+) in each image at an axial distance below the feed pipe of 0.015 m and 0.04 m, respectively.

pipe (0.008 m) and a radius of about 0.02 m, respectively. The frequency of a turbulent motion with  $r = 0.008$  m is 0.5 Hz, and the frequency of a turbulent motion with  $r = 0.02$  m is 1.6 Hz. These frequencies are calculated by substituting Eqs. 14 and 13 in Eq. 12, with a stirrer speed equal to 3 Hz and  $r$  equal to 0.008 m and 0.02 m, respectively. The frequency of the smallest turbulent motions causing the feed-

stream to oscillate ( $f_L$ ) is assumed to be equal to the average of these two frequencies, that is,  $f_L = 1$ .

A typical example of an energy spectrum calculated from tangential velocities measured at  $z = 0.05$  m below the feed pipe for a stirrer speed of 3.1 Hz is given in Figure 8. The value of the energy spectrum related to the large-scale oscillations [ $E_{i,LS}(f)$ ] has been approximated by the average of

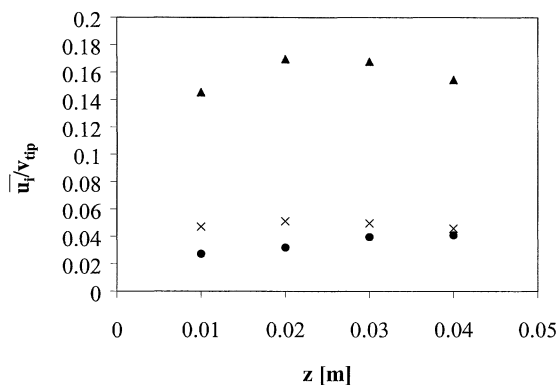


**Figure 6. Axial, tangential and radial mean velocities normalized by the tip velocity as a function of the axial coordinate below the feed pipe.**

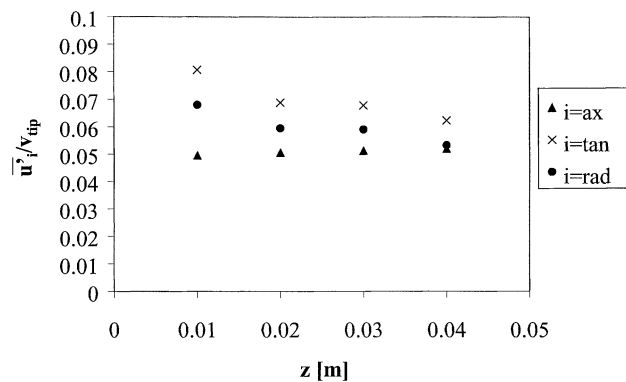


**Figure 7. Axial, tangential, and radial root mean square velocity fluctuations normalized by the tip velocity as a function of the axial coordinate below the feed pipe.**

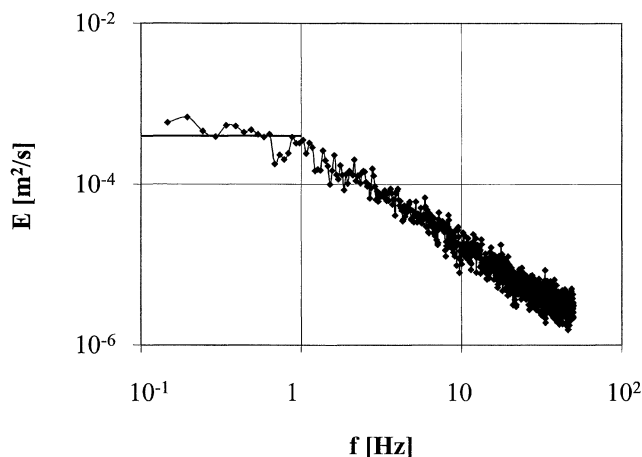


**Figure 8.** Energy spectrum calculated from tangential velocities measured at a distance of 0.05 m below the feed pipe and for a stirrer speed of 3 Hz.

the points obtained in the range  $0.1 \text{ Hz} < f \leq 1 \text{ Hz}$ . A typical example of  $E_{i,LS}(f)$  is given in Figure 8 by means of a horizontal line.

The velocity fluctuations in radial and tangential direction related to the large-scale turbulent motions are given in Figure 9. It is concluded from this figure that the square root of these velocity fluctuations in both directions are approximately equal to 0.03 times the tip velocity.

The X and Y coordinates of the centers-of-mass of a feedstream in a radial cross section at an axial distance of 0.025 m below the feed pipe for a stirrer speed of 3 Hz are given in Figure 10. The rms radius of the displacements is calculated from the X and Y coordinates, as given in Figure 10. In Figure 11 the rms radius of the displacements is given as a function of the axial distance from the feed pipe for stirrer speeds of 1.5, 3 and 4 Hz, respectively. No significant variation of the radius with impeller speed is observed in this figure.

In Figure 12 the rms radius of the displacements is given as a function of Lagrangian time for stirrer speeds of 1.5 Hz, 3

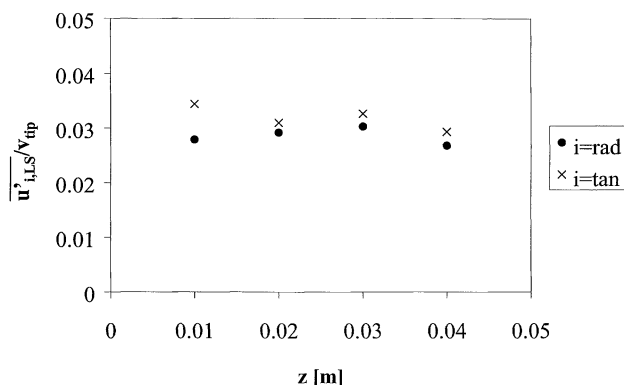


**Figure 9.** Velocity fluctuations related to the large-scale turbulent motions in radial and tangential direction normalized by the tip velocity as a function of the axial coordinate below the feed pipe.

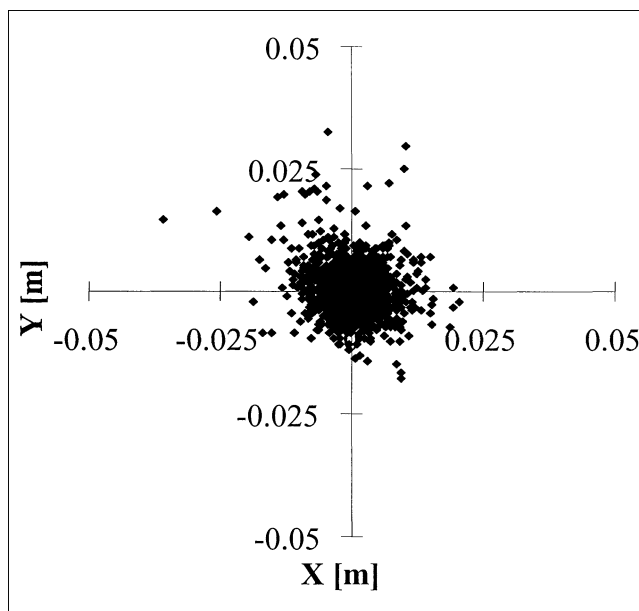


**Figure 10.** X and Y-coordinates of the centers of mass of a feedstream in a radial cross section at 0.025 m below the feed pipe and a stirrer speed of 3 Hz.

Hz, and 4 Hz, respectively. The Lagrangian time has been calculated with Eq. 9 with the average axial velocity equal to  $0.16v_{tip}$ . It is concluded from this figure that the rms radius is directly proportional to time, which corresponds to the “initial growth stage.”

The growth of the mean square radius of the displacements with time in the “initial growth stage” is given by Eq. 7. Substituting Eq. 9 for the Lagrangian time scale in Eq. 7, with the average velocity equal to  $0.16v_{tip}$  and the velocity fluctuations related to large-scale turbulent motions equal to  $0.03v_{tip}$ , yields the following equation for the rms radius of the displacements of the centers-of-mass ( $r_{cm}$ )

$$r_{cm} = \sqrt{u'^2_{rad,LS} + u'^2_{tan,LS}} \frac{z}{u_{ax}} = \sqrt{(0.03v_{tip})^2 + (0.03v_{tip})^2} \times \frac{z}{0.16v_{tip}} = 0.27z \quad (17)$$

with  $z$  is the axial distance below the feed pipe. From Eq. 17, follows that  $r_{cm}$  as a function of the axial distance below the feed pipe is independent of the stirrer speed, which is in agreement with the results shown in Figure 11.

The rms radius of the displacements of a passive marker ( $r_{pm}$ ) depends on the total velocity fluctuations in radial and tangential direction being equal to  $0.06v_{tip}$  and  $0.07v_{tip}$ , respectively

$$r_{pm} = \sqrt{u'^2_{rad} + u'^2_{tan}} \frac{z}{u_{ax}} = \sqrt{(0.06v_{tip})^2 + (0.07v_{tip})^2} \frac{z}{0.16v_{tip}} = 0.58z \quad (18)$$

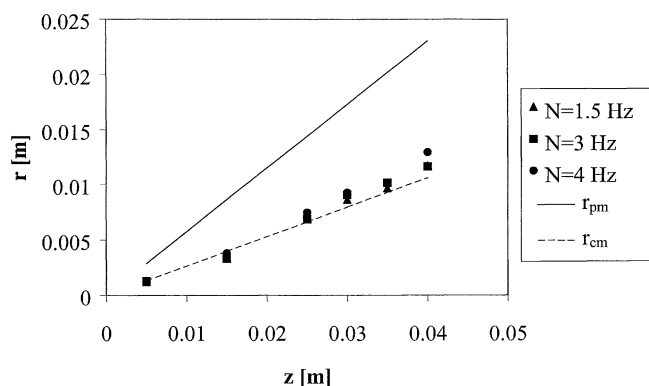


**Figure 11.** Measured root mean square (rms) radius of the center-of-mass of a feedstream for stirrer speeds of 1.5, 3, and 4 Hz, calculated rms radius of the centers-of-mass of a feedstream ( $r_{cm}$ ) and calculated rms radius of a passive marker ( $r_{pm}$ ) as a function of axial distance below the feed pipe.

Figure 11 shows comparisons between the measured rms radius of the displacements of the centers-of-mass  $r_{cm}$  calculated with Eq. 17 and  $r_{pm}$  calculated with Eq. 18 as a function of the axial distance below the feed pipe. This figure shows that the growth rate of  $r_{pm}$  equal to the total velocity fluctuations is much faster than the growth rate of the rms radius of the displacements of the centers-of-mass. A good agreement is obtained between the measured and calculated rms radius of the displacements of the centers-of-mass, when a growth rate is calculated with velocity fluctuations related only to large-scale turbulent motions. This supports our presumptions that large-scale turbulent motions are responsible for the oscillations of a feedstream in a stirred tank reactor.

## Conclusions and Practical Application

In this study, the increase of the root mean square radius of the displacements of the centers-of-mass of a feedstream

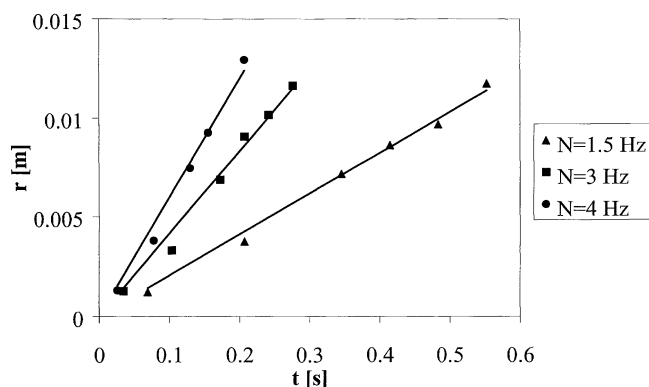


**Figure 12.** Root mean square radius of the centers of mass of a feedstream in radial cross sections as a function of a Lagrangian time scale for a stirrer speed of 1.5 Hz, 3 Hz, and 4 Hz, respectively.

with time is shown to be linear, which corresponds to the “initial growth stage.”

The rms radius grows as a function of time with a rate equal to the root of the sum of velocity fluctuations related to large-scale turbulent motions, which are apparently responsible for the oscillations of a feedstream in a stirred tank reactor.

In practice, the obtained description for the rms radius of the displacements of the centers-of-mass as a function of time can be used to calculate the minimal distance between feed pipes necessary to prevent the feedstreams from overlapping. This represents an important feature for the design and scale-up of stirred tank reactors with multiple feed points.

## Notation

$C$	= instantaneous tracer concentration
$C_{u_i u_i}$	= autocovariance of the velocity fluctuations
$D_{im}$	= impeller diameter
$E_i$	= energy spectrum
$f$	= frequency
$G$	= instantaneous gray value
$\bar{G}$	= average gray value
$N$	= impeller speed
$N_q$	= pumping capacity
$r$	= root mean square radius of the displacements
$r_c$	= circulation ratio
$t$	= time
$t_c$	= circulation time
$t_j$	= transit time
$T_L$	= Lagrangian time scale
$\bar{u}_i$	= mean velocity
$u'_{iL}$	= fluid velocity
$u_i'^2$	= mean square turbulent velocity fluctuations
$V_{reactor}$	= reactor volume
$v_{tip}$	= stirred tip speed
$X, Y$	= Cartesian positions
$\bar{X}^2$	= root mean square displacement
$z$	= axial distance below the feed pipe
$\Delta$	= spatial resolution
$\eta_j$	= transit time weighting factor
$\rho_{ii}$	= Lagrangian two time velocity autocorrelation coefficient

## Subscripts

ax	= axial
B	= background
$C_{hom}$	= tracer concentration in a homogeneous solution
cm	= center-of-mass
i	= coordinate direction
LS	= value for the large-scale energy eddies
pm	= passive marker
rad	= radial
SH	= sample hold
tan	= tangential
x	= x-direction
y	= y-direction
z	= z-direction
0	= initial value

## Literature Cited

- Adrian, R. J., and C. S. Yao, “Power Spectra of Fluid Velocities Measured by Laser Doppler Velocimetry,” *Exp. In Fluids*, **5**, 17 (1987).
- Baldyga, J., and J. R. Bourne, *Turbulent Mixing and Chemical Reactions*, Wiley, Chichester, U.K. (1999).

- Baldyga, J., J. R. Bourne, and S. J. Hearn, "Interaction between Chemical Reactions and Mixing on Various Scales," *Chem. Eng. Sci.*, **52**, 457 (1997).
- Baldyga, J., J. R. Bourne, and Yang Yang, "Influence of Feed Pipe Diameter on Mesomixing in Stirred Tank Reactors," *Chem. Eng. Sci.*, **48**, 3383 (1993).
- Blackadar, A. K., "Turbulence and Diffusion in the Atmosphere, Lectures in Environmental Sciences," *Springer-Verlag*, Berlin Heidelberg, 129 (1996).
- Houcine, I., E. Plasari, R. David, and J. Villiermaux, "Feedstream Jet Intermittency Phenomenon in a Continuous Stirred Tank Reactor," *Chem. Eng. J.*, **72**, 19 (1999).
- Houcine, I., H. Vivier, E. Plasari, R. David, and J. Villiermaux, "Planar Laser Induced Fluorescence Technique for Measurement of Concentration Fields in Continuous Stirred Tank Reactors," *Exp. in Fluids*, **22**, 95 (1996).
- Lesieur, M., *Turbulence in Fluids: Stochastic and Numerical Modeling*, Kluwer Academic Publishers, Dordrecht (1990).
- Rotta, J. C., *Turbulente Stromungen*, B. G. Teubner, Stuttgart (1972).
- Rys, P., "The Mixing-Sensitive Product Distribution of Chemical Reactions," *Chimia*, **46**, 469 (1992).
- Schoenmakers, J. H. A., J. G. Wijers, and D. Thoenes, "Determination of Feed Stream Mixing Rates in Agitated Vessels," *Proc. 8th Europ. Mix. Conf.: Récent Progrès en Génie des Procédés*, ed. Lavoisier, France, **52**, 185 (1997).
- Schoenmakers, J. H. A., "Turbulent Feed Stream Mixing in Agitated Vessels," PhD Thesis, Eindhoven University of Technology, The Netherlands (1998).
- Taylor, G. I., "Diffusion by Continuous Movements," *Proc. London Math. Soc.*, **20**, 196 (1921).
- Tennekes, H., and J. L. Lumley, *A First Course in Turbulence*, MIT Press, Cambridge (1972).
- Verschuren, I. L. M., J. G. Wijers, and J. T. F. Keurentjes, "Effect of Mixing on the Product Quality in Semi-Batch Stirred Tank Reactors," *AIChE J.*, **47**, 1731 (2001).
- Verschuren, I. L. M., J. G. Wijers, and J. T. F. Keurentjes, "Mean Concentrations and Concentration Fluctuations in a Stirred-Tank Reactor," *AIChE J.*, **48**, 1390 (2002).

Manuscript received May 10, 2001, and revision received Jan. 15, 2002.